Available online at www.sciencedirect.com

SciVerse ScienceDirect

journal homepage: www.elsevier.com/locate/he

Role of the composition and preparation method in the activity of hydrotalcite-derived Ru catalysts in the catalytic partial oxidation of methane

Adriana Ballarini [a,*], *Patricia Benito* [b,**], *Giuseppe Fornasari* [b], *Osvaldo Scelza* [a], *Angelo Vaccari* [b]

[a] *Instituto de Investigaciones en Catálisis y Petroquímica (INCAPE), FIQ – Universidad Nacional del Litoral – CONICET, Santiago del Estero 2654, S3000AOJ Santa Fe, Argentina*

[b] *Dipartimento di Chimica Industriale "Toso Montanari", Alma Mater Studiorum, Università di Bologna, Viale Risorgimento 4, 40136 Bologna, Italy*

ARTICLE INFO

Article history:
Received 6 June 2013
Received in revised form
6 August 2013
Accepted 29 August 2013
Available online 11 October 2013

Keywords:
Ruthenium
Hydrotalcite
Methane
H_2 production
Syngas
Catalytic partial oxidation

ABSTRACT

Hydrotalcite-derived Ru catalysts were tested in the catalytic partial oxidation of CH_4 to produce syngas. The effect of Ru content, oxidic matrix composition, and preparation procedure on chemical–physical properties and performances of catalysts was studied. Bulk catalysts (0.25 and 0.50 wt.% Ru) were obtained via Ru/Mg/Al hydrotalcite-type (HT) precursors with carbonates or silicates as interlayer anions. A supported catalyst was prepared by impregnation on a calcined Mg/Al–CO_3 HT. Ru/γ-Al_2O_3 was evaluated for comparison. Both the Ru dispersion and the interaction with the support decreased as the Ru loading increased and when silicates were present due to RuO_2 segregation. Regardless of the Ru loading, carbonate-derived catalysts performed better than those containing silicates. The increased Ru loading improved the initial activity, but deactivation occurred after high temperature tests. Stability tests for shorter contact times over a 0.25 wt.% bulk sample obtained from Ru/Mg/Al HT with carbonates showed a tendency to deactivate at 750 °C.

1. Introduction

In addition to its applications in the chemical industry, H_2 is considered to be the major energy carrier of the future, whereas syngas (CO and H_2) can be used for chemical, fuel and power production. Although many efforts are directed toward H_2 and syngas production from renewable sources, natural gas is still the main industrial scale raw material [1]. To improve the already existing natural gas-based processes, research is focused on finding solutions for both lower investment costs and the use of an autothermic process. On these bases, an optimum solution for replacing the steam reformers is the catalytic partial oxidation (CPO) of methane, a mild exothermic process that operates at short contact times [2,3]. For instance, small reactors with fast startups and shutdowns can be used for the small-scale production of H_2 [4]. Moreover, the H_2/CO molar ratio obtained is around 2, suitable for hydrocarbon synthesis by Fischer–Tropsch

* *Corresponding author*. Tel.: +54 (342) 4571164; fax: +54 (342) 4531068.
** *Corresponding author*. Tel.: +39 0512093677; fax: +39 0512093679.
E-mail addresses: adriballa@hotmail.com (A. Ballarini), patricia.benito3@unibo.it (P. Benito).

0360-3199/$ – see front matter
http://dx.doi.org/10.1016/j.ijhydene.2013.08.135

reaction in gas to liquid processes [5]. Nevertheless, there are some constraints to the application of this process: the reaction temperature may be difficult to control due to the formation of hot spots, resulting in effects on process safety and catalyst deactivation. Thus catalysts must be chemically and mechanically stable at high gas-hourly space velocity (GHSV) values and prevent the formation of hot spots.

Rh catalysts are very active in the CPO of methane [2,3]; however, the reduced availability and high cost of Rh could make it unsuitable for widespread commercial applications. Ru is less expensive than Rh and is active in the conversion of CH_4, not only by partial oxidation [2,3] but also in dry and steam reforming reactions [6,7] as well as in combined dry-partial oxidation processes [8]. Moreover, Ru reduces the deactivation by carbon deposition [9]. For application in the partial oxidation of methane, Ru was deposited by the conventional impregnation procedure on Al_2O_3 [10,11], TiO_2 [12–14], SiO_2 [15,16], ZrO_2 modified with TiO_2 [17], Nb_2O_5–ZrO_2, Ta_2O_5–ZrO_2 [18] and Y_2O_3 [19]. Catalysts were used in both pelletized and structured forms, such as membrane reactors [20] and monoliths [21]. Polycrystalline Ru-supported metal nanoparticles have a high relative chemical activity, being easily oxidized and reduced [22]. In the CPO process it has been observed that the oxidation state and, therefore, the activity and selectivity depend on both the reaction conditions and the nature of the support [10,14,23]. For instance, Ru on SiO_2 deactivates very rapidly, and Ru/Al_2O_3 has good activity and selectivity, while the mixture CeO_2–ZrO_2 leads to low selectivity toward partial oxidation products [24]. On the other hand, Ru/TiO_2 catalysts show high selectivity to syngas since the interaction between Ru and TiO_2 prevents the oxidation of Ru during reaction [12–14]. The easy oxidation of Ru metal in comparison to Rh when supported on Al_2O_3 [11] and SiO_2 [16] is due to the greater M–O bond strength of the Ru–O bond compared with the Rh–O one. The formation of RuO_2 decreases the activity toward CPO, thus fostering the total oxidation. Moreover, at high temperatures volatile RuO_4 species may be formed [25], yielding to further catalyst deactivation [24].

Several studies have been devoted to increasing the activity and stability of Ru catalysts. A Ru/Al_2O_3 catalyst was prepared by deposition of colloidal Ru particles [23] and microemulsion [21], while the support was modified by doping with Ce [26]. Furthermore, to stabilize Ru at high temperature, bulk catalysts were used. In the early 1990s Ashcroft et al. reported that bulk ruthenate pyrochlores were active in the CPO, but they were not stable under CPO conditions [27,28]. Recently the stability of Ru in the pyrochlore structure was improved by partially substituting the Ru metal in the structure of lanthanum–strontium–zirconate, and catalysts were tested in the CPO of diesel surrogate [29] and CO_2 reforming [30]. Ru-substituted hexa-aluminates prevent the volatilization of Ru after calcination at high temperatures and reaction conditions by means of the strong interaction between Ru and the base oxide [31,32]. Lastly, bulk Ru catalysts obtained from hydrotalcite-type compounds have been used in the CPO [33,34] and dry reforming [35] of CH_4.

Hydrotalcite-type (HT) compounds are layered materials with the general chemical formula $[M^{2+}_{1-x}M^{3+}_{x}(OH)_2]\ (A^{n-})_{x/n}\ nH_2O$ that are used as catalyst precursors [36]. Catalysts are obtained by thermal treatment at high temperatures (around 900 °C). In particular, to prepare Ru catalysts for the CPO of CH_4, Ru/Mg/Al–CO_3 HT compounds were synthesized [33,34]. A Rietveld characterization of high loaded catalysts revealed that after calcination Ru is incorporated into the MgO matrix and segregated as RuO_2; the M^{2+}/M^{3+} ratio modifies the distribution of Ru and the catalytic performances [34]. The A^{n-} anions in the interlayer region are usually carbonates, but silicates may also be intercalated to improve the mechanical stability of the final catalysts [37]. The advantage of using HT as precursors for CPO catalysts lies in the fact that their thermal activation leads to mixed oxides, with a relatively large specific surface area, high thermal stability, and dispersion of the active species [37]. Moreover, the metal-support interaction is stronger than in catalysts obtained by the usual impregnation or deposition methods. However, the amount of available active species may be lower than the actual metal loading, because some of them may be "trapped" inside the bulk of the solid. Takehira and co-workers have reported the incorporation of noble metals in mixed oxides obtained by calcination of HT compounds by the so-called memory effect [38,39].

The aim of this work was to develop stable and active catalysts operating in the CPO both at high and low temperatures. Thus HT-derived Ru catalysts were synthesized to study the effect of Ru loading, oxide matrix composition, and preparation procedure on the chemical–physical properties and performances of catalysts. Low loaded bulk and supported catalysts were prepared both to reduce the cost of the catalyst and to stabilize the Ru in the oxidic matrix, while avoiding the segregation of RuO_2. Bulk catalysts were prepared by the conventional method involving coprecipitation of the HT precursor followed by calcination. Ru/Mg/Al-HT precursors containing carbonates or silicates in the interlayer region were synthesized to improve both the catalytic performances and the mechanical stability. Lastly, impregnated catalysts were also prepared to increase the amount of Ru on the surface. The incipient wetness impregnation was performed on supports derived from Mg/Al–CO_3 HT precursors calcined at 900 °C, in order to decrease the tendency of the structure to reconstruct. For comparison purposes a conventional supported a Ru/γ-Al_2O_3 catalyst was evaluated. The activity of catalysts was studied not only by feeding diluted gas mixtures, as in the case of most of the above-mentioned works, but also with concentrated gas mixtures to evaluate the stability of the samples.

2. Materials and methods

2.1. Preparation of the catalysts

2.1.1. Coprecipitation: b-Ru(0.25 and 0.50)-exHT-CO_3 and b-Ru(0.25 and 0.50)-exHT-sil

Ru-HT precursors [Ru/Mg/Al = 0.1/80/19.9 and 0.25/80/19.75 atomic ratio (a.r.)] containing carbonates (b-HT-CO_3) and silicates (b-HT-sil) were prepared by coprecipitation at constant pH. A solution containing nitrates of the cations ($RuCl_3$, 41 wt.% Ru, $Mg(NO_3)_2{\cdot}6H_2O$, and $Al(NO_3)_3{\cdot}9H_2O$) in the appropriate ratios was slowly added to a solution containing carbonates (Na_2CO_3) or silicates (sodium silicate solution,

NaOH ≥ 10%, SiO_2 ≥ 27%, Aldrich). pH was kept constant at 10.5 ± 0.2 by the dropwise addition of NaOH. The slurry obtained was aged under vigorous stirring at 60 °C for 45 min. After washing, the precipitate was dried overnight at 60 °C. Catalysts were obtained by calcination at 900 °C for 12 h (heating rate 10 °C min^{-1}). The precursors of the catalysts were labeled: b-Ru(X)-HT-Y, where X is the Ru loading in wt.% and Y is the anion in the HT precursor, i.e. CO_3^{2-} or sil, for instance, b-Ru(0.25)-HT-CO_3 and b-Ru(0.25)-HT-sil. To name samples after calcination, the word "ex" was added before HT, namely b-Ru(0.25)-exHT-CO_3 and b-Ru(0.25)-exHT-sil.

2.1.2. *Impregnation: i-Ru(0.25)/exHT-CO_3*

Ru-supported catalysts (0.25 wt.%) were prepared using a calcined Mg/Al HT-CO_3 precursor. The support was obtained by calcination at 900 °C for 12 h of a Mg/Al HT compound (Mg/Al = 80/20 as a.r.) containing carbonates and synthesized by following the same procedure as reported above. The support (exHT-CO_3) was impregnated with a solution of Ru (III) chloride hydrate (41 wt.% Ru) for 6 h at 25 °C and dried overnight at 60 °C. The solution volume/support weight ratio was 1.5 mL g^{-1}. After the impregnation (sample i-Ru(0.25)/exHT-CO_3 IWI), the catalyst was calcined at 500 °C for 3 h. The catalyst was labeled i-Ru(0.25)/exHT-CO_3.

2.1.3. *Impregnation: Ru(0.25)/Al_2O_3*

Ruthenium catalyst (0.25 wt.%) was prepared by using a commercial γ-Al_2O_3 (Cynamid Ketjen CK-300) with S_{BET} = 190 m^2 g^{-1} and V_{pore} = 0.5 cm^3 g^{-1}, which was impregnated by a solution of Ru (III) chloride hydrate (41 wt.% Ru). The impregnation was obtained using a solution with a volume/support weight ratio of 1.4 mL g^{-1}. Lastly, the catalyst was calcined at 500 °C for 3 h. This catalyst was named Ru(0.25)/Al_2O_3.

2.2. *Catalytic tests*

Catalytic tests were carried out in a quartz reactor (i.d. 8 mm) filled with 0.5 g of catalyst. The pellet particle size was between 0.60 and 0.42 mm to avoid pressure drop, giving a bed length of approximately 2 cm. The reactor was inserted into an electric oven. The gas-phase temperature was measured by a chromel-alumel thermocouple sliding on a quartz wire inside the catalyst bed. The catalytic tests aimed to study the sample activity and stability toward deactivation by sintering, oxidation, and coke formation. The partial oxidation reaction was carried out at 500 °C and 750 °C oven temperature and several gas mixtures were fed into the reactor for different contact times: CH_4/O_2/He v/v = 2/1/20 (65 and 35 ms), 2/1/40 (35 ms), 2/1/4 (65 ms) and 2/1/1 (55 ms). Tests were done at higher oven temperatures with concentrated gas mixtures to study the deactivation of samples. In the low temperature tests, the presence of large amounts of He made it possible to decrease the effect of the heat evolved in the reaction and better discern the activity of the investigated samples. Catalysts were reduced in situ at 750 °C in an equimolar H_2/N_2 mixture (7 L/h) for 12 h. Reaction products were analyzed online, after water condensation, by a Perkin Elmer gas chromatograph equipped with two HWD and Carbosieve SII columns, using He as carrier gas for the analysis of CH_4, O_2, CO, and CO_2 and N_2 for the analysis of H_2. Oxygen was consumed completely in all the catalytic tests. The conversion of CH_4 and selectivity to H_2 and CO were calculated according to the formulas 1, 2, and 3 below:

$$\text{Conv. } CH_4 = \frac{F_{CH_4}\text{in} - F_{CH_4}\text{out}}{F_{CH_4}\text{in}} * 100 = \frac{F_{CO}\text{out} + F_{CO_2}\text{out}}{F_{CO}\text{out} + F_{CO_2}\text{out} + F_{CH_4}\text{out}} * 100 \quad (1)$$

$$\text{Sel. } H_2 = 0.5 * \frac{F_{H_2}\text{out}}{F_{CO}\text{out} + F_{CO_2}\text{out}} * 100 \quad (2)$$

$$\text{Sel. CO} = \frac{F_{CO}\text{out}}{F_{CO}\text{out} + F_{CO_2}\text{out}} * 100 \quad (3)$$

Reaction conditions were set for 2 h and the values here reported were the average of the obtained values.

The catalyst displaying the best catalytic performance in the above-reported tests was subjected to long-term experiments. Catalytic tests were performed for a short contact time (5 ms), by loading 0.1 g of catalyst into the quartz reactor. The following reaction conditions were set: i) Toven = 750 °C, CH_4/O_2/He = 2/1/4 v/v; ii) Toven = 500 °C, CH_4/O_2/He = 2/1/4, 2/1/20 and 2/1/40 v/v.

2.3. *Characterization of the catalysts*

Powder X-Ray Diffraction (PXRD) analyses were carried out using a Philips PW1050/81 diffractometer equipped with a graphite monochromator and controlled by a PW1710 unit (CuKα-Ni filtered, λ = 0,15418 nm). A 2θ range from 5° to 80° was investigated at a scanning rate of 70°h^{-1}. Specific surface area and pore volume measurements were done using a Micromeritics ASAP 2020 instrument. Samples were previously degassed under vacuum by heating at 250 °C for 30 min before the N_2 adsorption.

The characteristics of metallic particles were determined by Cyclohexane Dehydrogenation (CHD) test reaction, Transmission Electron Microscopy (TEM), Temperature-Programmed Reduction (TPR), and X-Ray Photoelectron Spectroscopy (XPS), and the quantification of the carbonaceous deposits by Temperature-Programmed Oxidation (TPO) using thermogravimetric analysis (TGA).

The CHD test reaction of the metallic phase was carried out in a differential flow reactor with a 26H_2/CH molar ratio. The reaction temperature was 400 °C. Samples were previously reduced at 750 °C for 12 h. Reaction products were analyzed by gas chromatography with a FID detector.

Temperature-programmed reduction (TPR) experiments were carried out in a quartz flow reactor. Samples (0.300 g) were heated at 6 °C min^{-1} from room temperature (r.t.) up to 950 °C. The reduction mixture H_2 (5% (v/v)/N_2) was fed to the reactor with a flow rate of 10 mL min^{-1}.

Transmission electron micrographs of reduced and used Ru containing catalysts were taken by using a JEOL 100CX microscope with a nominal resolution of 6 Å, operated with an acceleration voltage of 100 KV, and magnification ranges of 80,000× and 100,000×. Samples were introduced into the microscope column; for each catalyst, a significant number of Ru

particles were observed and the distribution curves of particle sizes plotted.

XPS measurements were carried out in a Specs spectrometer, which operates with an energy power of 50 eV (radiation Mg Kα, hν = 1253.6 eV at high binding energy). The pressure of the analysis chamber was kept at 4.10^{-10} torr. Samples were previously reduced under similar reaction conditions as those of the catalytic reactor and then introduced into the analysis chamber and reduced "in situ" with H_2 at 300 °C for 1 h to clean the catalyst surfaces. Spectral regions corresponding to C1s, O1s, Mg2s, Al2p, Ru3d, and Ru3p core levels were recorded for each sample. Ru3d and C1s peaks overlapped at 284 eV, and the binding energies (B.E.) were referred to the C1s peak. The C1s peak was subtracted from the original spectrum. Peak areas were estimated by fitting the experimental results with Lorentzian–Gaussian curves by using the CASA XPS software. XPS quantification in terms of peak intensity is performed by assigning quantification regions. The relative sensitivity factor, labeled RSF, for the peak intensity is applied. Finally, %Atomic Concentrations were obtained for each region.

To quantify carbonaceous deposits, the profiles of temperature-programmed oxidation (TPO) in catalysts before and after the CPO reaction were determined by using the thermogravimetric analysis (TGA) technique. Experiments were carried out on the SDTA Mettler STAR^e. Fresh (used as a reference) and used catalysts were stabilized under N_2 flow at 250 °C for 1 h before starting the TPO experiments. Samples (0.010 g) were heated at 5 °C min^{-1} from 250 °C to 900 °C under air flow.

3. Results and discussion

3.1. Characterization of the HT precursors and catalysts

X-ray diffractograms of HT-precursors, bulk and supported 0.25 wt.% Ru catalysts are shown in Fig. 1(a) and (b). The diffraction patterns of HT precursors containing carbonates (b-HT-CO_3) show characteristic lines of a hydrotalcite structure [36]. After calcination at 900 °C (Fig.1(a)), XRD patterns show peaks corresponding to MgO-type (JCPDS 45-0946) and $MgAl_2O_4$-type phases (JCPDS 5-0672). Diffractograms of bulk catalysts with a different Ru loading, namely b-Ru(0.25)-exHT-CO_3 and b-Ru(0.50)-exHT-CO_3, are similar. Silicate-intercalated samples (b-HT-sil) have less intense and broader peaks (Fig. 1(b)) thus suggesting a decrease in the crystallinity of the solids as compared to b-HT-CO_3 samples; moreover, the structure of b-Ru(0.25)-exHT-sil and b-Ru(0.50)-exHT-sil catalysts Fig. 1(b)) was modified. After calcination, the formation of a magnesium silicate (Mg_2SiO_4) phase with an olivine structure (JCPDS 4-0768) and the incomplete crystallization of the spinel phase are the main differences from the catalysts obtained from the b-HT-CO_3 precursors [40]. A small peak is identified at around 28.1° in the XRD pattern of the sample with a higher Ru

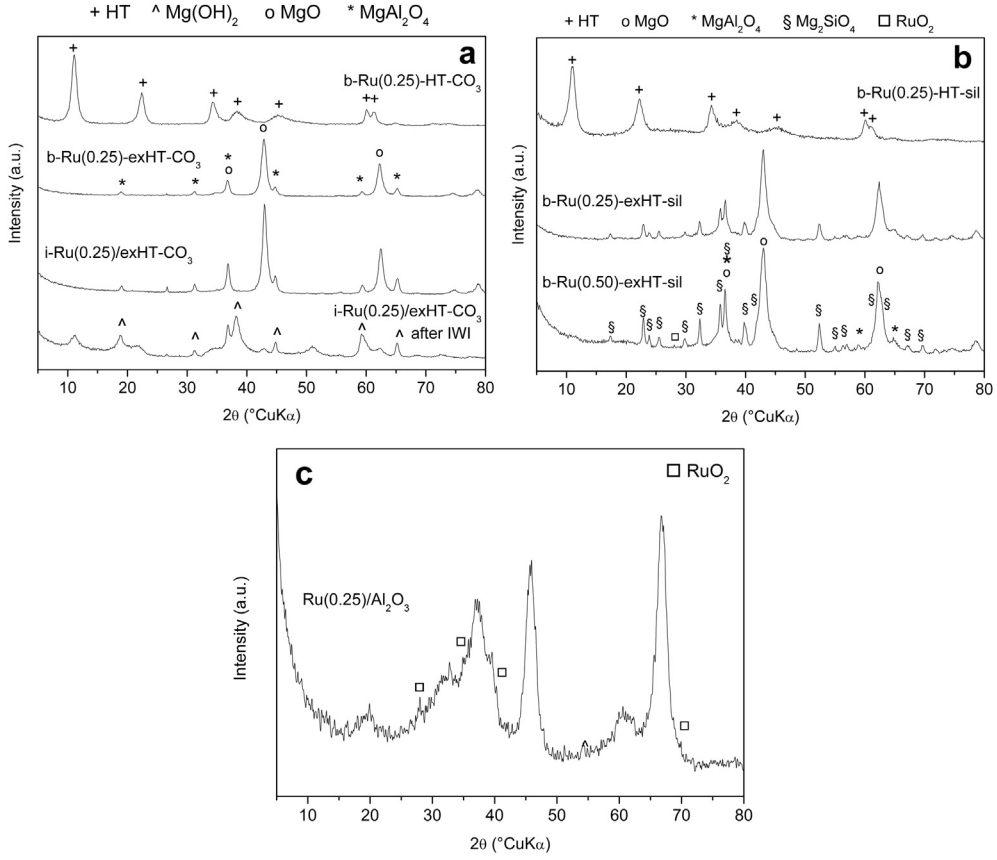

Fig. 1 – Powder XRD patterns of HT precursors, bulk and impregnated catalysts: a) HT-CO_3 samples; b) HT-sil samples; c) Ru(0.25)/Al_2O_3.

Table 1 – Specific surface area values (S_{BET}) of supports, fresh and used catalysts prepared by coprecipitation and impregnation.

Supports	Catalysts	S_{BET} ($m^2 g^{-1}$)	
		Fresh	Used
exHT-CO_3		103	
	i-Ru(0.25)/exHT-CO_3 (IWI)	95	
	i-Ru(0.25)/exHT-CO_3	134	93
	b-Ru(0.25)-exHT-CO_3	95	106
	b-Ru(0.25)-exHT-sil	95	103
Al_2O_3		190	
	Ru(0.25)/Al_2O_3	220	166

loading, b-Ru(0.50)-exHT-sil (Fig. 1(b)), ascribed to the (110) line of the RuO_2 tetragonal rutile phase. Ru atoms may be distributed in the MgO-type phase and segregated RuO_2 [33]; thus it appears that the presence of silicates alters the distribution Ru species with respect to the samples obtained from b-HT-CO_3.

With regard to the preparation method, the XRD pattern of the supported i-Ru(0.25)/exHT-CO_3 catalyst is quite similar to the pattern of the corresponding b-Ru(0.25)-exHT-CO_3 bulk catalyst (Fig. 1(a)). However, it is worth noting that during the incipient wetness impregnation some structural changes occur. After drying the impregnated sample (i-Ru(0.25)/exHT-CO_3 IWI, Fig. 1(a)), peaks due to the spinel phase remain almost constant, whereas MgO peaks decrease; furthermore, $Mg(OH)_2$ and HT structures are formed. Therefore, the reconstruction of hydroxides occurred, despite the high calcination temperature of the HT precursor (900 °C) [41]. In Fig. 1(c), the XRD pattern of the Ru(0.25)/Al_2O_3 catalyst shows characteristic diffraction peaks at $2\theta = 38$, 45 and 67° (JCPDS 10-0425) corresponding to γ-Al_2O_3 and – unlike the HT-derived samples – some small diffraction peaks due to the rutile RuO_2 phase (JCPDS 40-1290).

Table 1 summarizes the BET surface area values of both supports and fresh catalysts. There are no significant differences between bulk samples prepared from b-HT-CO_3 or b-HT-sil precursors. Specific surface area values around 100 $m^2 g^{-1}$ have been measured. On the other hand, the i-Ru(0.25)/exHT-CO_3 supported catalyst shows a slightly larger specific surface area (134 $m^2 g^{-1}$) than the coprecipitated one (95 $m^2 g^{-1}$). This may be due to both the reconstruction during impregnation and the softer thermal treatment after impregnation (500 °C vs 900 °C).

Mg/Al ratio values on the catalyst surface were estimated from XPS analysis on 0.25 wt.% Ru-loaded samples (Table 2). The Mg/Al ratio obtained for the b-Ru(0.25)-exHT-CO_3 sample is close to the expected bulk catalyst composition. Conversely, the value decreases when silicates are introduced in the structure of the catalysts or for the supported sample.

Fig. 2 shows TPR profiles of bulk and supported catalysts. The reduction profile of Ru(0.25)/Al_2O_3 (Fig. 2(a)) is similar to those reported in the literature [42,43]. It is made of two relatively sharp peaks with maximum at 210 °C and 250 °C, and a broad low-intensity high-temperature reduction band at 400 °C. The low temperature reduction peaks may be attributed to the reduction of well-dispersed RuO_x and bulk RuO_2 species [42]. The broad band may be assigned to the reduction of oxidized Ru species interacting strongly with Al_2O_3 [43]. TPR profiles of HT-derived catalysts slightly depend on the Ru loading and oxidic matrix composition. Both for bulk and supported 0.25 wt.% catalysts, b-Ru(0.25)-exHT-CO_3, b-Ru(0.25)-exHT-sil and i-Ru(0.25)/exHT-CO_3 (Fig. 2(a)), a very small H_2 consumption is recorded at around 265 °C, and the main reduction occurs at higher temperatures (around 438 °C and 467 °C). The intensity of the low temperature peak increases in 0.50 wt.% samples, b-Ru(0.50)-exHT-CO_3, b-Ru(0.50)-exHT-sil, with respect to the high temperature ones (Fig. 2(b)). Thus it could be stated that in 0.25 wt.% loaded catalysts only a small amount of ruthenium is segregated as RuO_2, which is not detected by XRD, whereas most of the oxidized ruthenium species are well-stabilized in the catalyst matrix. Similar reduction peaks have been reported in literature for Ru/MgO–Al_2O_3 catalysts, attributed to the reduction of strongly interacting RuO_2 species formed at the interface between the metal and the support [7]. The high reduction temperature peak observed in the i-Ru(0.25)/exHT-CO_3 impregnated sample could be explained by the partial reconstruction of HT and $Mg(OH)_2$ phases during impregnation, while involving the incorporation of ruthenium species in the hydroxides. The peak shifted toward lower temperatures with respect to the bulk catalyst, thus suggesting either a larger metallic particle size or a lower interaction with the support. The latter behavior may be explained by either the lower thermal treatment temperature of the sample after IWI or the different number of Mg- and Al-containing species involved in the structure reconstruction, since both effects modify the phases in which the Ru species may be distributed. In the sample containing silicates (b-Ru(0.25)-exHT-sil) the reduction profile is similar to that described for the b-Ru(0.25)-exHT-CO_3 catalyst, but the main H_2 consumption is recorded at lower temperatures. The formation of the forsterite phase reduces the amount of Mg available for the formation of the MgO phase, wherein ruthenium species may be dispersed, thus reducing their stability. This effect is more notable in 0.50 wt.% loaded catalysts (Fig. 2(b)). As previously stated, RuO_2 is segregated in both catalysts, but the reduction occurred at a lower temperature in the b-Ru(0.50)-exHT-sil catalyst, thus indicating that a larger amount of Ru species are present as segregated RuO_2, in agreement with XRD data.

Reduced Ru catalysts were characterized by cyclohexane dehydrogenation test reaction (CHD) and XPS analysis. The

Table 2 – Binding energies (BE) and surface atomic ratios obtained by XPS of Ru catalysts after reduction on H_2.

Catalysts	Ru3$d_{5/2}$	XPS surface atomic ratio	Surface atomic ratio
	BE (eV)	Mg/Al	Ru^0/RuO_2
b-Ru(0.25)-exHT-CO_3	279.4 Ru (0) 284.2 Ru (IV)	4.05	0.52
i-Ru(0.25)/exHT-CO_3	279.2 Ru (0) 284.3 Ru (IV)	2.90	0.51
b-Ru(0.25)-exHT-sil	279.3 Ru (0) 284.5 Ru (IV)	3.20	0.77
Ru(0.25)/Al_2O_3	279.1 Ru (0) 284.3 Ru (IV)	–	0.20

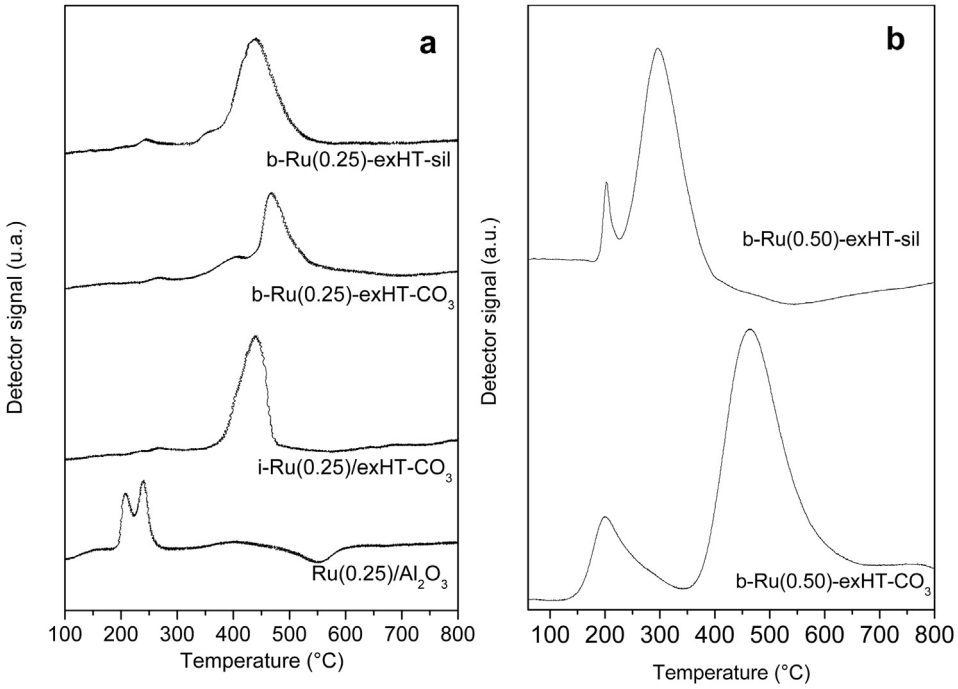

Fig. 2 – TPR profiles of (a) 0.25 wt.% Ru loaded catalysts: b-Ru(0.25)-exHT-Sil, b-Ru(0.25)-exHT-CO_3, i-Ru(0.25)/exHT-CO_3, and Ru(0.25)/Al_2O_3 and (b) 0.50 wt.% Ru loaded catalysts: b-Ru(0.50)-exHT-Sil, b-Ru(0.50)-exHT-CO_3.

CHD is structure-insensitive and depends on the fraction of exposed active metal: it could therefore be considered an indirect measure of metal dispersion [44,45]. However, for the HT-derived catalysts, CHD could be considered only as a measure of the exposed Ru metal sites. Apparent activation energy and initial reaction rates (R^0CH) of CHD are summarized in Table 3. The initial reaction rate of CHD is slightly higher for the bulk b-Ru(0.25)-exHT-CO_3 than for the impregnated i-Ru(0.25)/exHT-CO_3 catalyst. On the other hand, activation energy values are similar regardless of the preparation method (about 20 kcal/mol). It would appear that the bulk catalyst contains a larger amount of exposed Ru atoms that lead to a faster reaction rate; but the interaction between the active metal and support does not depend on the preparation procedure, because the activation energy is not modified. For the b-Ru(0.25)-exHT-sil catalyst prepared from silicate precursors, the dehydrogenating activity (18 mol/h $g_{catalyst}$) is greater, showing a larger amount of exposed Ru atoms than the b-Ru(0.25)-exHT-CO_3 sample. On the other hand, the activation energy of CHD is similar to that of the previously commented catalysts. Lastly, the Ru(0.25)/Al_2O_3 catalyst, resulting from the segregation of RuO_2, shows a higher activation energy value and a lower initial reaction rate in CHD than the catalysts prepared from HT compounds.

Table 3 – Apparent activation energy and initial reaction rates (R^0CH) of CHD for Ru catalysts at 400 °C.

Catalyst	Apparent activation energy (kcal/mol)	R^0 CH (mol/h $g_{catalyst}$)
b-Ru(0.25)-exHT-CO_3	21	12
i-Ru(0.25)/exHT-CO_3	20	9
b-Ru(0.25)-exHT-sil	20	18
Ru(0.25)/Al_2O_3	43	<1

In order to thoroughly investigate the metallic phase on the catalyst surface, Ru(3d) spectra were obtained by XPS measurements on reduced samples. The XPS spectra obtained in the Ru(3d) region of the catalysts prepared from HT precursors were very similar. They consisted of a doublet with a Ru($3d_{5/2}$) BE at about 279.0 eV, which is characteristic of metal Ru(0), and a second doublet attributed to Ru(IV) species at about 284.4 eV [13,46]. The constraints used in the spectral analysis regarding the ratio between the areas of the Ru($3d_{5/2}$) and Ru($3d_{3/2}$) peaks and their BE difference give a satisfactory fitting of the signal shape that registered in both doublets. The C1s peak that corresponds to the contamination carbon was subtracted from the original spectrum. The main Ru $3p_{3/2}$ peak at 461.2 eV clearly indicates that most of ruthenium in both catalysts was in a metallic form [13,14,47,48]. Ru $3d_{5/2}$ binding energies and surface atomic ratios Ru/RuO_2 are shown in Table 2. Ru/RuO_2 ratios are similar in b-Ru(0.25)-exHT-CO_3 and i-Ru(0.25)/exHT-CO_3 catalysts prepared via a carbonate precursor regardless of the synthesis procedure (coprecipitation or impregnation). The surface atomic ratio of the catalyst b-Ru(0.25)-exHT-sil is higher than those of the above-mentioned catalysts due to the increased amount of Ru^0 present, in agreement with the CHD results. Moreover, the ratio increases for the b-Ru(0.50)-exHT-CO_3 sample (0.67) in comparison to the b-Ru(0.25)-exHT-CO_3 sample (0.52). However it must be noted that the presence of Ru^{4+} species may be related to the metallic Ru particles covered by an oxide film. Therefore the differences observed among catalysts may be related to the different degree of oxidation [48].

Table 4 – Outlet temperature (T_{out}) and maximum reaction temperature (T_{max}) of the gas phase measured by thermocouple for the b-Ru(0.25)-exHT-CO_3.

CH_4/O_2/He (v/v)	2/1/20		2/1/20		2/1/4		2/1/1		2/1/20		2/1/20		2/1/40	
τ (ms)	65		65		65		55		65		35		35	
Toven (°C)	500		750		750		750		500		500		500	
Sample	T_{out}	T_{max}	T_{out}	T_{max}	T_{out}	T_{max}	T_{out}	T_{max}	T_{out}	T_{max}	T_{out}	T_{max}	T_{out}	T_{max}
b-Ru(0.25)-exHT-CO_3	540	585	753	769	780	830	815	894	540	582	579	625	546	580

A similar spectrum is obtained for the Ru(0.25)/Al_2O_3 catalyst with a Ru $3d_{5/2}$ peak at 279.1 eV, which is attributed to Ru^0 metallic species. An additional $3d_{5/2}$ peak around 284.3 eV was also found, which can be attributed to the presence of oxidized Ru species. Similar results were reported by several authors [14,46–49]. What is more, the Ru(0.25)/Al_2O_3 catalyst had a lower Ru/RuO_2 ratio compared to the catalysts prepared by HT precursors due to formation of larger metallic particles with a lower amount of Ru^0 exposed, as revealed by the CHD test reaction, although the formation of RuO_2 species could not be ruled out.

3.2. *Catalytic activity*

The catalytic behavior (CH_4 conversion, selectivity in CO, and H_2) of the samples depends on the Ru loading, chemical composition of the support, and preparation procedure. However, the general trend observed with different reaction conditions is similar to those previously reported for Ni and Rh catalysts obtained from HT precursors [37]. The temperature inside the catalyst bed varied depending on the reaction conditions, while the temperature at the outlet of the catalytic bed (T_{out}) and the maximum temperature (T_{max}) were recorded for every catalyst. In Table 4, the temperatures measured for b-Ru(0.25)-exHT-CO_3 catalyst are summarized as an example.

At first, both the effect of Ru-loading and the nature of HT precursor (b-HT-CO_3 and b-HT-sil) on the activity and stability of the catalysts were studied. Figs. 3 and 4 summarize the most significant performances of 0.25 wt.% and 0.50 wt.% Ru loaded bulk catalysts at different reaction conditions (temperature and CH_4/O_2/He volume ratios). The initial catalytic test, at an oven temperature of 500 °C and while feeding a diluted gas mixture (CH_4/O_2/He = 2/1/20 v/v), was used to highlight the different activities in freshly reduced samples (Fig. 3(a)). Methane conversion was low (50–60%) and the syngas was rich in H_2, due to the significant contribution of the water gas shift (WGS) reaction. Oxygen conversion was always complete. Regardless of the Ru loading, reduced bulk catalysts obtained from b-HT-CO_3 compounds (b-Ru(0.25)-exHT-CO_3 and b-Ru(0.50)-exHT-CO_3) were more active and selective to syngas than catalysts containing silicates (b-Ru(0.25)-exHT-sil and b-Ru(0.50)-exHT-sil). However, in a series of samples the higher the Ru loading was, the better the catalytic performances were.

Performances were improved by increasing the oven temperature to 750 °C, as expected by the thermodynamic equilibrium [26]; while CH_4 conversion, selectivity in CO, and H_2 depended on the composition of the gas mixture. Under the most favorable reaction conditions, namely at low reactant partial pressure (CH_4/O_2/He = 2/1/20 v/v), CH_4 conversion was about 96% for all the catalysts, H_2 and CO being the main products (selectivity over 95%). By feeding concentrated CH_4/O_2/He = 2/1/4 and 2/1/1 v/v gas mixtures, especially with the latter (Fig. 4), the performances obtained with b-Ru(0.25)-exHT-CO_3 and b-Ru(0.50)-exHT-CO_3 catalysts were slightly better than those achieved with b-Ru(0.25)-exHT-sil and b-Ru(0.50)-exHT-sil catalysts. These results confirm that catalysts obtained from b-HT-CO_3 are more active than those prepared from b-HT-sil. Lastly, the stability of catalysts was studied by repeating the initial test after high temperature reaction conditions (Fig. 3(b)). A loss of activity was observed for both highly loaded catalysts and the b-Ru(0.25)-exHT-sil sample, while the b-Ru(0.25)-exHT-CO_3 catalyst improved its activity with respect to the initial test.

The role of the preparation method (coprecipitation or impregnation) and nature of the support (exHT-CO_3 or γ-Al_2O_3) on the performances of 0.25 wt.% loaded samples was studied in a second step (Figs. 5 and 6). In the test at an oven temperature of 500 °C and feeding the CH_4/O_2/He = 2/1/20 v/v mixture (Fig. 5(a)), the impregnation method gave rise, regardless of the support, to freshly reduced i-Ru(0.25)/exHT-CO_3 and Ru(0.25)/Al_2O_3 catalysts with poorer activity than the

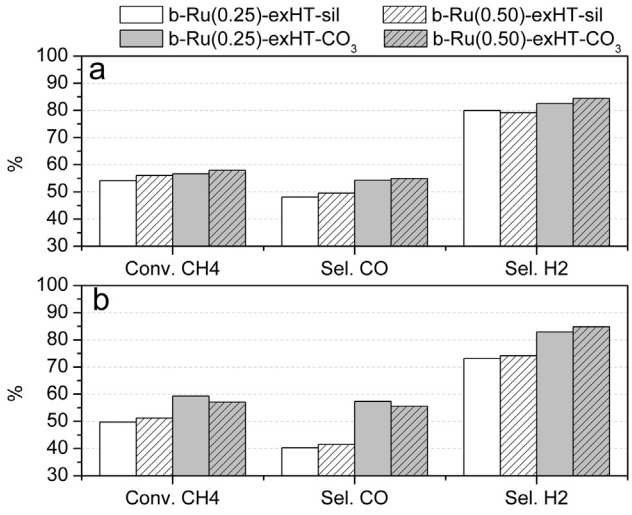

Fig. 3 – Methane conversion and selectivities in H_2 and CO for 0.25 and 0.50 wt.% Ru loaded bulk catalysts, b-Ru(0.25)-exHT-CO_3, b-Ru(0.50)-exHT-CO_3, b-Ru(0.25)-exHT-sil, b-Ru(0.50)-exHT-sil, at CH_4/O_2/He = 2/1/20 v/v and 500 °C: a) initial test, b) repeated test after high temperature reaction conditions.

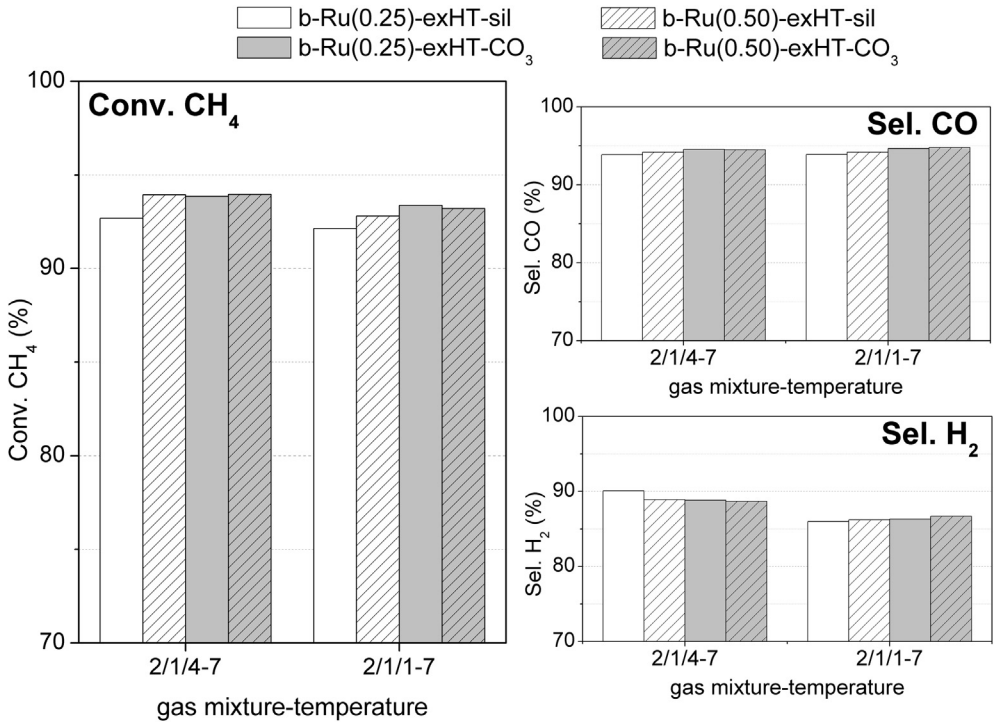

Fig. 4 – Methane conversion and selectivities in H_2 and CO for 0.25 and 0.50 wt.% Ru loaded bulk catalysts, b-Ru(0.25)-exHT-CO_3, b-Ru(0.50)-exHT-CO_3, b-Ru(0.25)-exHT-sil, b-Ru(0.50)-exHT-sil, at 750 °C and CH_4/O_2/He = 2/1/4 and 2/1/1 v/v.

b-Ru(0.25)-exHT-CO_3 bulk sample. The differences in the catalytic activity may be due to metal dispersion, the stability of Ru(0) species to oxidation, and carbon deposition. By taking into account the characterization results, the lower activity of the Ru(0.25)/Al_2O_3 sample supported on γ-Al_2O_3 may be due to both a lower Ru dispersion and the oxidation of the Ru metal [10,13,23]; moreover, the acidity of the support may promote the deactivation by carbon deposition (see below). The catalytic trend of the b-Ru(0.25)-exHT-CO_3 and i-Ru(0.25)/exHT-CO_3 samples obtained from HT precursors does not fit perfectly with the amount of available Ru sites obtained in CHD tests, thus the oxidation of the metallic particles, mainly at the entrance of the catalyst bed, may play a key role in the activity at the low oven temperature [10,13,23]. Oxidized catalysts promote total oxidation: in fact the maximum temperature (measured at the inlet of the catalyst bed) is higher for i-Ru(0.25)/exHT-CO_3 and Ru(0.25)/Al_2O_3 samples (603 and 605 °C respectively).

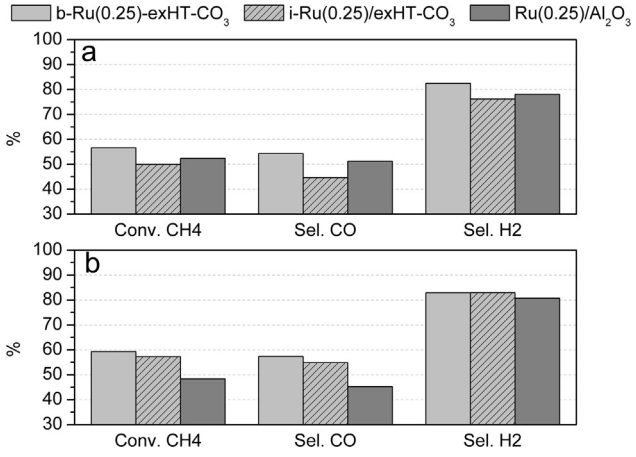

Fig. 5 – Methane conversion and selectivities in H_2 and CO values for Ru 0.25 wt.%. catalysts as a function of preparation methods (coprecipitation vs impregnation) or nature of the support (exHT-CO_3 or Al_2O_3), b-Ru(0.25)-exHT-CO_3, i-Ru(0.25)/exHT-CO_3, Ru(0.25)/Al_2O_3, operating at CH_4/O_2/He = 2/1/20 v/v and 500 °C: a) initial test, b) repeated test after high temperature reaction conditions.

When the oven temperature was raised to 750 °C (Fig. 6(a)), during the 2/1/20 *v/v* test, the activity of the i-Ru(0.25)/exHT-CO_3 catalyst was closer to that of the b-Ru(0.25)-exHT-CO_3 bulk catalyst. The Ru(0.25)/Al_2O_3 sample still shows a lower conversion (87%) but the selectivity to H_2 is high (Fig. 6(b)). By feeding concentrated CH_4/O_2/He = 2/1/4 and 2/1/1 *v/v* gas mixtures, the different performances between bulk and supported catalysts were reduced. The temperature inside the catalyst bed increased (see Table 4), thus affecting the catalytic activity. Moreover, the activation of the catalysts may take place due to the reduction of the RuO_2 formed during the tests at low temperature, since the oxidation state of ruthenium depends on the reaction temperature [10,13,23]. By repeating the test in the initial condition (Fig. 5(b)), Ru(0.25)/Al_2O_3 deactivated, whereas i-Ru(0.25)/exHT-CO_3 similarly activated as the bulk b-Ru(0.25)-exHT-CO_3 catalyst. The increase and stabilization of the catalytic activity at high temperature has been reported to be significant for the activity of noble metals at low temperature [50].

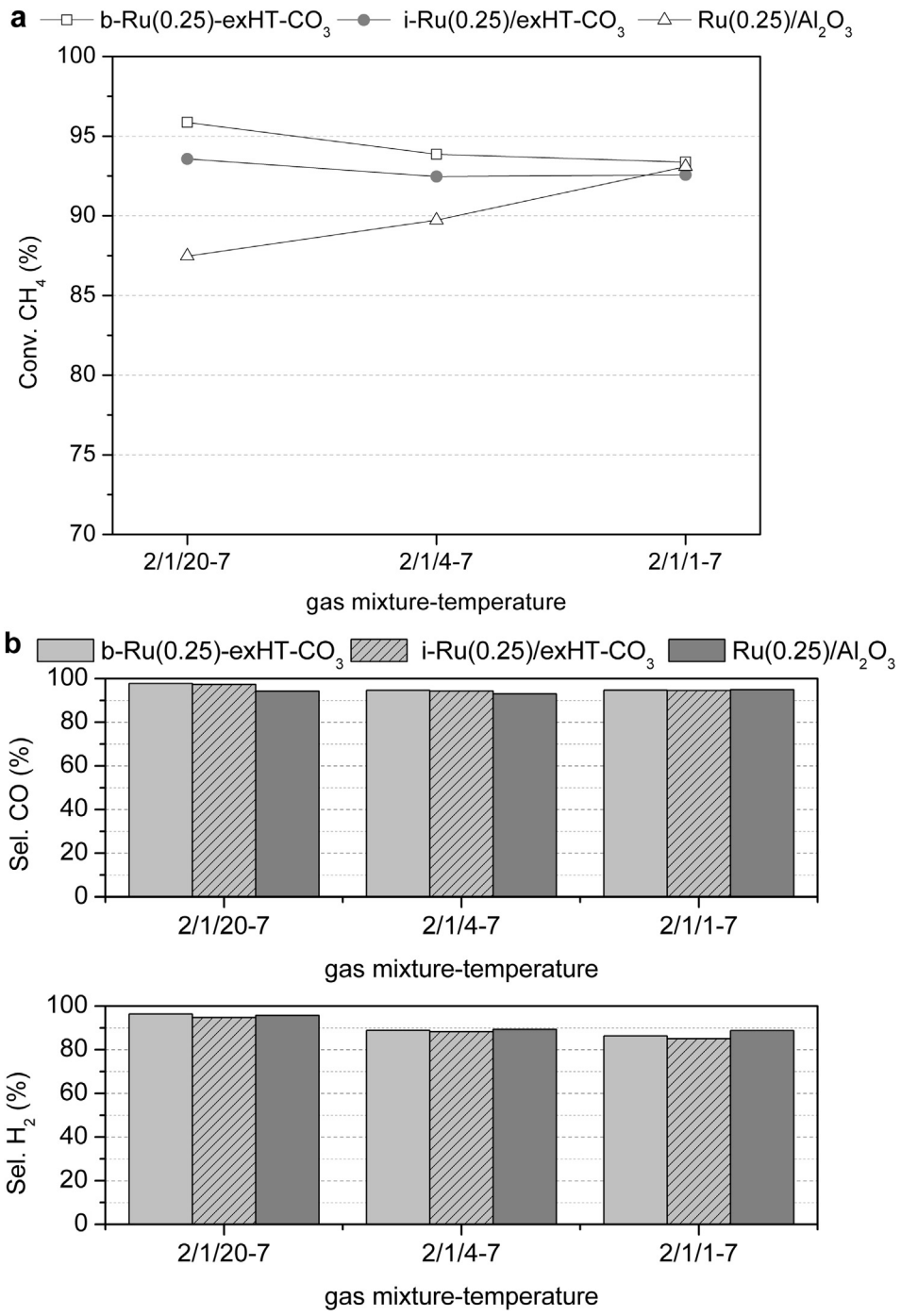

Fig. 6 – Methane conversion (a) and selectivities in H_2 and CO (b) for b-Ru(0.25)-exHT-CO_3, i-Ru(0.25)/exHT-CO_3, Ru(0.25)/Al_2O_3 catalysts operating at 750 °C and CH_4/O_2/He = 2/1/20; 2/1/4 and 2/1/1 v/v.

Lastly, the effect of the contact time on CH_4 conversion and syngas selectivity during tests at 500 °C was further studied for 0.25 wt.% loaded catalysts, b-Ru(0.25)-exHT-CO_3, i-Ru(0.25)/exHT-CO_3, and Ru(0.25)/Al_2O_3 (Fig. 7). The activity was evaluated at 35 ms by feeding the reactor with 2/1/20 and 2/1/40 *v/v* gas mixtures. When changing from 65 to 35 ms of contact time, CH_4 conversion and selectivity in CO highly increased, whereas smaller differences were found in the selectivity in H_2. The increase in temperature is responsible for better performances (Table 4), and is more notable for the Ru(0.25)/Al_2O_3 catalyst, as previously reported for tests at 750 °C. The effect of the heat developed within the bed decreased by increasing the dilution degree (Table 4). Performances were only slightly higher than in the 2/1/20–5 test at 65 ms and no modifications in the activity order were observed. Therefore, catalytic tests for shorter contact times confirmed the above-reported trend in the activity of the catalysts.

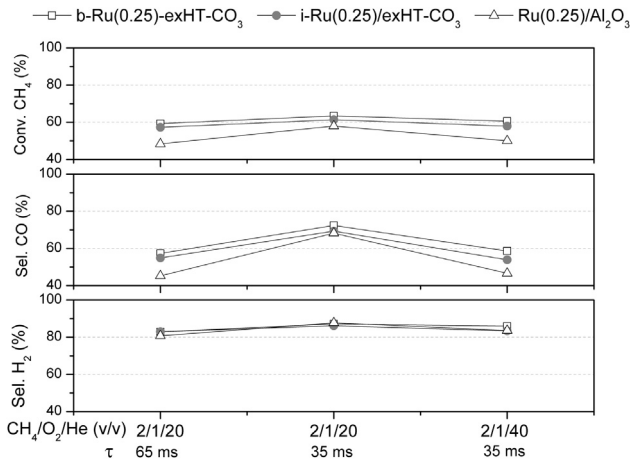

Fig. 7 – Methane conversion and selectivities in H_2 and CO values for b-Ru(0.25)-exHT-CO_3, i-Ru(0.25)/exHT-CO_3, Ru(0.25)/Al_2O_3 catalysts operating at 500 °C and CH_4/O_2/He = 2/1/20; 2/1/40 v/v.

3.3. *Characterization of used catalysts*

To study the deactivation/activation mechanisms taking place with time-on-stream, post-reaction catalysts were characterized. XRD patterns of catalysts obtained from HT-derived catalysts were not modified after the catalytic tests; only small Ru(0) reflections were identified in the b-Ru(0.50)-exHT-sil catalyst. On the other hand, θ- and γ-Al_2O_3 phases and small peaks of Ru(0) were identified in the diffraction pattern of the Ru(0.25)/Al_2O_3 catalyst. The high temperatures reached in the catalyst bed promoted the phase transition and the sintering of the metallic particles. Table 1 shows the specific surface area values (S_{BET}) of the used catalysts. S_{BET} values of bulk HT-derived catalysts remain fairly close to the values of fresh catalysts, thus confirming their good thermal stability. However, the S_{BET} of i-Ru(0.25)/exHT-CO_3 catalyst decreased after the catalytic tests, due to the lower thermal stability of the support and/or sintering of the metallic phase which decrease the pore volume. The surface area of the Ru(0.25)/Al_2O_3 catalyst decreased greatly from 220 $m^2\ g^{-1}$ to 166 $m^2\ g^{-1}$, in agreement with the phase changes observed in the XRD data commented on herein before.

The carbon deposition on the catalyst surface during tests was studied by TPO. The basic character of oxides [36] in HT-derived catalysts prepared by coprecipitation or impregnation prevented the carbon formation, since the analysis performed gives a C content below the detection limit. On the other hand, Ru(0.25)/Al_2O_3 showed a small amount of C (0.15% C). It must be noted that γ-Al_2O_3 has Lewis acidity [51], so the small amount of carbon may be attributed to the acidity of the support.

The best-performing catalyst, b-Ru(0.25)-exHT-CO_3, was further analyzed by TEM. Metallic particles of sizes ranging from 2 to 10 nm, with mean particle size of around 4–5 nm, were observed in the reduced fresh sample. The Ru(0) size of the particles was slightly increased after catalytic tests (mean particle size 5.25 nm), thus confirming the good stability of this sample under reaction conditions. However, it should be mentioned that Ru nanoparticles smaller than 2–3 nm may form RuO_2 in ambient conditions [49]; thus the presence of smaller particles cannot be ruled out.

Taking into account the catalyst characterization before and after the tests may help explain some of the catalytic behaviors. The deactivation of Ru(0.25)/Al_2O_3 is related to the sintering of support and metallic particles, as well as to carbon formation, as previously reported [10]. With regard to HT-derived catalysts, the segregation of RuO_2 and their further sintering or oxidation is responsible for the loss in activity of 0.50 wt.% Ru-loaded and silicate-containing catalysts, b-Ru(0.50)-exHT-CO_3, b-Ru(0.25)-exHT-sil, and b-Ru(0.50)-exHT-sil. As for the synthesis procedure, the reconstruction of the structure during Ru impregnation led to well dispersed and stable metallic particles in i-Ru(0.25)/exHT-CO_3 catalysts, in spite of the fact that the catalyst is less active than the corresponding b-Ru(0.25)-exHT-CO_3 bulk sample. The activation observed for both catalysts after tests at high temperature could be related to the reduction of RuO_2 species; however, for the i-Ru(0.25)/exHT-CO_3 catalyst, the biggest difference between the initial and final tests under the same conditions suggests a reorganization of the metallic particles. Namely, metallic particles in the initial tests were more easily oxidized than in the final one. Fresh catalysts may be supposed to have smaller particles than the catalysts after high temperature reaction, the latter being more stable against oxidation [6,23,52]. This effect is more evident for the impregnated catalysts, because of the lower calcination temperature, which determines the Ru/support interaction and the particle size.

3.4. *Long-term catalytic tests*

Long-term catalytic tests were carried out for a shorter contact time (5 ms), with the catalyst showing the best performances (b-Ru(0.25)-exHT-CO_3) to test its stability. The short contact time was achieved by loading a small amount of catalyst (0.1 g vs 0.5 g) and increasing the inlet flow rate, so the heat transfer within the catalyst bed could be altered. Performances were evaluated at T_{oven} = 750 °C by feeding the CH_4/O_2/He = 2/1/4 *v/v*

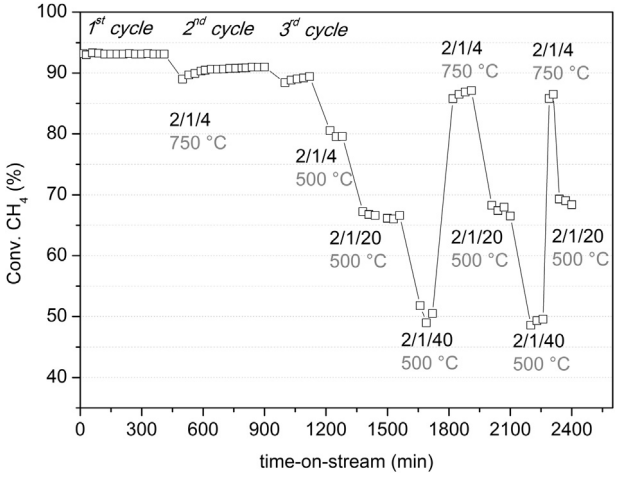

Fig. 8 – Methane conversion values during long-term catalytic tests on b-Ru(0.25)-exHT-CO_3 catalyst for a short contact time (5 ms).

gas mixture and at $T_{oven} = 500\ ^{\circ}C$ by feeding both concentrated and diluted gas mixtures ($CH_4/O_2/He$ = 2/1/4, 2/1/20 and 2/1/40 v/v). The effect of shutdown and startup cycles on performances was also studied. CH_4 conversion values are summarized in Fig. 8.

In the test at 750 °C, high CH_4 conversion (93%) and selectivity in H_2 and CO are achieved and remained constant at 7 h of time-on-stream. Then the shutdown and startup were performed in He atmosphere by decreasing the oven temperature to room temperature and raising it to 750 °C. After the first shutdown, the initial conversion was approximately 89%, but the catalyst was activated in the first 120 min, reaching a constant value of about 91%. The same behavior was observed after the second shutdown, with a final conversion of 89%. It appears that the shutdown and startup play a key role in the deactivation mechanism.

After the tests at 750 °C, the activity of the catalyst was studied at 500 °C by feeding 2/1/4, 2/1/20, and 2/1/40 v/v gas mixtures. The catalyst was very active when feeding the 2/1/4 v/v reaction mixture, reaching 80% conversion of CH_4. The heat evolved by exothermic reactions justifies this high activity. However, it appears that both water gas shift and reforming reactions are fostered less under these reaction conditions, since the selectivity to CO (92%) is greater than selectivity to H_2 (88%). The dilution of the mixture reduced the amount of heat generated in the bed, and therefore lowered the CH_4 conversion from 65% to 50% for the 2/1/20 and 2/1/40 v/v gas mixtures, respectively.

To determine whether the deactivation is due to the shutdown and startup, two further reaction cycles were performed at $T_{oven} = 750\ ^{\circ}C$ and 500 °C for 120 min. Performances remained rather constant at both temperatures; it is possible to observe what was previously mentioned about the activation with time-on-stream during tests at high temperature. The catalyst deactivation is measured by DP values, defined as $DP = 100 \cdot (X_0 - X_f)/X_0$, (where X_0 and X_f are the initial and the final CH_4 conversions). The DP was greatest (4%) between the 1st and 2nd cycle, and 1.4% between the 2nd and 3rd cycle. The total deactivation in the short contact time was about 10% between the 1st and last cycle. These results suggest that the catalyst is stable during the shutdown and startup, although high temperatures for long reaction times deactivate it slightly.

4. Conclusions

The activity and stability of Ru-catalysts derived from HT precursors in the CPO of CH_4 depend on the Ru loading (0.5 and 0.25 wt.%), intercalated anions in the HT (carbonates or silicates), and synthesis procedure (coprecipitation or impregnation). The classic coprecipitation method, for the synthesis of Ru/Mg/Al HTs, leads to bulk catalysts in which both the inclusion of silicates in the structure and the increase of the Ru loading (regardless of the anions) foster the segregation of RuO_2 and therefore deactivation after tests at high temperature and 65–55 ms. For low loaded catalysts (0.25 wt.% Ru), the reconstruction of the $Mg(OH)_2$ and HT structures during impregnation improves the metal-support interaction in comparison to a traditional Ru/γ-Al_2O_3, but the catalyst is less active than the corresponding bulk sample obtained from Ru/Mg/Al–CO_3. The higher activity and stability of the 0.25 wt.% catalyst derived from Ru/Mg/Al–CO_3 during tests at high temperatures and 65–55 ms is due to an enhanced metal–support interaction, carbon resistance, and thermal stability. However, a slight deactivation is observed when it is tested for a very short contact time (5 ms) at high temperature.

Acknowledgments

Authors thank Miguel Torres for his experimental assistance. This work was performed in the frame of ERASMUS MUNDUS Project, Cooperation Window, Line 6. The financial support by the Ministero per l'Università e la Ricerca (MIUR, Italy), the Consejo Nacional de Investigaciones Científicas y Técnicas (CONICET, Argentina), Universidad Nacional del Litoral (Argentina) and ANPCyT are gratefully acknowledged.

REFERENCES

[1] Liu K, Song C, Subramani V, editors. Hydrogen and syngas production and purification technologies. Hoboken, New Jersey: John Wiley & Sons, Inc.; 2010.
[2] Enger BC, Lødeng R, Holmen A. A review of catalytic partial oxidation of methane to synthesis gas with emphasis on reaction mechanisms over transition metal catalysts. Appl Catal A 2008;346:1–27.
[3] Liu K, Deluga GD, Bitsch-Larsen A, Schmidt LD, Zhang L. In: Liu K, Song C, Subramani V, editors. Hydrogen and syngas production and purification technologies. Hoboken, New Jersey: John Wiley & Sons, Inc.; 2010. p. 127–55.
[4] Ferreira-Aparicio P, Benito MJ, Sanz JL. New trends in reforming technologies: from hydrogen industrial plants to multifuel microreformers. Catal Rev 2005;47:491–588.
[5] Perego C, Bortolo R, Zennaro R. Gas to liquids technologies for natural gas reserves valorization: the Eni experience. Catal Today 2009;142:9–16.
[6] Kehres J, Jakobsen JG, Andreasen JW, Wagner JB, Liu H, Molenbroek A, et al. Dynamical properties of a Ru/$MgAl_2O_4$ catalyst during reduction and dry methane reforming. J Phys Chem C 2012;116:21407–15.
[7] Carvalho LS, Martins AR, Reyes P, Oportus M, Albonoz A, Vicentini V, et al. Preparation and characterization of Ru/MgO–Al_2O_3 catalysts for methane steam reforming. Catal Today 2009;142:52–60.
[8] Nematollahi B, Rezaei M, Khajenoori M. Combined dry reforming and partial oxidation of methane to synthesis gas on noble metal catalysts. Int J Hydrogen Energy 2011;36:2969–78.
[9] Rostrup-Nielsen JR, Hansen JHB. CO_2-Reforming of methane over transition metals. J Catal 1993;144:38–49.
[10] Rabe S, Nachtegaal M, Vogel F. Catalytic partial oxidation of methane to synthesis gas over a ruthenium catalyst: the role of the oxidation state. Phys Chem Chem Phys 2007;9:1461–8.
[11] Liu Y, Huang FY, Li JM, Weng WZ, Luo CR, Wang ML, et al. In situ Raman study on the partial oxidation of methane to synthesis gas over Rh/Al_2O_3 and Ru/Al_2O_3 catalysts. J Catal 2008;256:192–203.
[12] Boucouvalas Y, Zhang Z, Verykios XE. Partial oxidation of methane to synthesis gas via the direct reaction scheme over Ru/TiO_2 catalyst. Catal Lett 1996;40:189–95.

[13] Elmasides C, Kondarides DI, Neophytides SG, Verykios XE. Partial oxidation of methane to synthesis gas over Ru/TiO_2 catalysts: effects of modification of the support on oxidation state and catalytic performance. J Catal 2001;198:195–207.
[14] Elmasides C, Kondarides DI, Grünert W, Verykios XE. XPS and FTIR study of Ru/Al_2O_3 and Ru/TiO_2 catalysts: reduction characteristics and interaction with a Methane–Oxygen mixture. J Phys Chem B 1999;103:5227–39.
[15] Weng WZ, Yan QG, Luo CR, Liao YY, Wan HL. The concentration of oxygen species over SiO_2-supported Rh and Ru catalysts and its relationship with the mechanism of partial oxidation of methane to synthesis gas. Catal Lett 2001;74:37–43.
[16] Yan QG, Wu TH, Weng WZ, Toghiani H, Toghiani RK, Wan HL, et al. Partial oxidation of methane to H_2 and CO over Rh/SiO_2 and Ru/SiO_2 catalysts. J Catal 2004;226:247–59.
[17] Choque V, Ramírez de la Piscina P, Molyneux D, Homs N. Ruthenium supported on new TiO_2–ZrO_2 systems as catalysts for the partial oxidation of methane. Catal Today 2010;149:248–53.
[18] Choque V, Homs N, Cicha-Szot R, Ramírez de la Piscina P. Study of ruthenium supported on Ta_2O_5–ZrO_2 and Nb_2O_5–ZrO_2 as catalysts for the partial oxidation of methane. Catal Today 2009;142:308–13.
[19] Nishimoto H, Nakagawa K, Ikenaga N, Suzuki T. Partial oxidation of methane to synthesis gas over Ru-loaded Y_2O_3. Catal Lett 2002;82:161–7.
[20] Paturzo L, Gallucci F, Basile A, Pertici P, Scalera N, Vitulli G. Partial oxidation of methane in a catalytic ruthenium membrane reactor. Ind Eng Chem Res 2003;42:2968–74.
[21] Lanza R, Canu P, Järås SG. Microemulsion-prepared ruthenium catalyst for syngas production via methane partial oxidation. Appl Catal A Gen 2008;337:10–8.
[22] Over H. Surface chemistry of ruthenium dioxide in heterogeneous catalysis and electrocatalysis: from fundamental to applied research. Chem Rev 2012;112:3356–426.
[23] Balint I, Miyazaki A, Aika Ki. The relevance of Ru nanoparticles morphology and oxidation state to the partial oxidation of methane. J Catal 2003;220:74–83.
[24] Lanza R, Järås SG, Canu P. Partial oxidation of methane over supported ruthenium catalysts. Appl Catal A Gen 2007;325:57–67.
[25] Ji L, Lin J, Zeng HC. Thermal processes of volatile RuO_2 in nanocrystalline Al_2O_3 matrixes involving $\gamma \rightarrow \alpha$ phase transformation. Chem Mater 2001;13:2403–12.
[26] Rabe S, Truong TB, Vogel F. Low temperature catalytic partial oxidation of methane for gas-to-liquids applications. Appl Catal A Gen 2005;292:177–88.
[27] Ashcroft AT, Cheetham AK, Foord JS, Green MLH, Grey CP, Murrell AJ, et al. Selective oxidation of methane to synthesis gas using transition metal catalysts. Nature 1990;344:319–21.
[28] Ashcroft AT, Cheetham AK, Jones RH, Natarajan S, Thomas JM, Waller D, et al. An in situ, energy-dispersive x-ray diffraction study of natural gas conversion by carbon dioxide reforming. J Phys Chem 1993;97:3355–8.
[29] Haynes DJ, Campos A, Berry DA, Shekhawat D, Roy A, Spivey JJ. Catalytic partial oxidation of a diesel surrogate fuel using an Ru-substituted pyrochlore. Catal Today 2010;155:84–91.
[30] Gaur S, Pakhare D, Wu H, Haynes DJ, Spivey JJ. CO_2 reforming of CH_4 over Ru-substituted pyrochlore catalysts: effects of temperature and reactant feed ratio. Energy Fuels 2012;26:1989–98.
[31] Kikuchi R, Iwasa Y, Takeguchi T, Eguchi K. Partial oxidation of CH_4 and C_3H_8 over hexaaluminate-type oxides. Appl Catal A Gen 2005;281:61–7.
[32] Bukhtiyarova MV, Ivanova AS, Slavinskaya EM, Kuznetsov PA, Plyasova LM, Stonkus O, et al. Steam reforming of methane over Ni-substituted Sr hexaaluminates. Catal Sustain Energy Res 2012;1:11–21.
[33] Basile F, Fornasari G, Gazzano M, Vaccari A. Rh, Ru and Ir catalysts obtained by HT precursors: effect of the thermal evolution and composition on the material structure and use. J Mater Chem 2002;12:3296–303.
[34] Basile F, Fornasari G, Rosetti V, Trifirò F, Vaccari A. Effect of the Mg/Al ratio of the hydrotalcite-type precursor on the dispersion and activity of Rh and Ru catalysts for the partial oxidation of methane. Catal Today 2004;91–92:293–7.
[35] Tsyganok AI, Inaba M, Tsunoda T, Hamakawa S, Suzuki K, Hayakawa T. Dry reforming of methane over supported noble metals: a novel approach to preparing catalysts. Catal Commun 2003;4:493–8.
[36] Cavani F, Trifirò F, Vaccari A. Hydrotalcite-type anionic clays: preparation, properties and applications. Catal Today 1991;11:173–301.
[37] Basile F, Benito P, Fornasari G, Vaccari A. Hydrotalcite-type precursors of active catalysts for hydrogen production. Appl Clay Sci 2010;48:250–9.
[38] Takehira K. Preparation of supported metal catalysts starting from hydrotalcites as the precursors and their improvements by adopting "memory effect". Catal Surv Asia 2007;11:1–30.
[39] Tsyganok AI, Inaba M, Tsunoda T, Suzuki K, Takehira K, Hayakawa T. Combined partial oxidation and dry reforming of methane to synthesis gas over noble metals supported on Mg–Al mixed oxide. Appl Catal A Gen 2004;275:149–55.
[40] Arpentinier P, Basile F, Del Gallo P, Fornasari G, Gary D, Rosetti V, et al. Role of the hydrotalcite-type precursor on the properties of CPO catalysts. Catal Today 2005;99:99–104.
[41] Rocha J, del Arco M, Rives V, Ulibarri MA. Reconstruction of layered double hydroxides from calcined precursors: a powder XRD and ^{27}Al MAS NMR study. J Mater Chem 1999;9:2499–503.
[42] Betancourt P, Rives A, Hubaut R, Scott CE, Goldwasser J. A study of the ruthenium–alumina system. Appl Catal A Gen 1998;170:307–14.
[43] Wang M, Weng W, Zheng H, Yi X, Huang C, Wan H. Oscillations during partial oxidation of methane to synthesis gas over Ru/Al_2O_3 catalyst. J Nat Gas Chem 2009;18:300–5.
[44] Cinneide AD, Clarke JKA. Catalysis on supported metals. Catal Rev 1972;7:213–32.
[45] Boudart M. Catalysis by supported metals. Adv Catal 1969;20:153–66.
[46] Wagner MCD, Riggs WM, Davis LE, Moulder JF, Muilenberg GE. Handbook of X-ray photoelectron spectroscopyIn Phys Electr. Perkin-Elmer Co.; 1979.
[47] Sanchez MA, Mazzieri V, Sad M, Grau R, Pieck C. Influence of preparation method and boron addition on the metal function properties of Ru–Sn catalysts for selective carbonyl hydrogenation. J Chem Technol Biotechnol 2011;86:447–53.
[48] Mazzieri V, Coloma-Pascual F, Arcoya A, L'Argentiere PC, Fígoli NS. XPS, FTIR and TPR characterization of Ru/Al_2O_3 catalysts. Appl Surf Sci 2003;210:222–30.
[49] Tsisum E, Nefedov B, Shpiro E, Antoshin G, Minachev K. XPS studies of Ru in γ-Al_2O_3 supported catalysts. React Kinet Catal Lett 1984;24:37–41.
[50] Jakobsen JG, Jørgensen TL, Chorkendorff I, Sehested J. Steam and CO_2 reforming of methane over a Ru/ZrO_2 catalyst. Appl Catal A Gen 2010;377:158–66.
[51] Pines H, Haag WO. Alumina: catalyst and support. I. Alumina, its intrinsic acidity and catalytic activity. J Am Chem Soc 1960;82:2471–8.
[52] Qadir K, Joo SH, Mun BS, Butcher DR, Renzas JR, Aksoy F, et al. Intrinsic relation between catalytic activity of co oxidation on Ru nanoparticles and Ru oxides uncovered with ambient pressure XPS. Nano Lett 2012;12:5761–8.